

\mathcal{F} -EBM: Energy Based Learning of Functional Data

Jen Ning Lim¹, Sebastian Vollmer^{1,2,3}, Lorenz Wolf⁴, and Andrew Duncan^{4,5}

¹University of Warwick

²University of Kaiserslautern

³DFKI, German Research Center for Artificial Intelligence

⁴Imperial College London

⁵The Alan Turing Institute

February 7, 2022

Abstract

Energy-Based Models (EBMs) have proven to be a highly effective approach for modelling densities on finite-dimensional spaces. Their ability to incorporate domain-specific choices and constraints into the structure of the model through composition make EBMs an appealing candidate for applications in physics, biology and computer vision and various other fields. In this work, we present a novel class of EBM which is able to learn distributions of functions (such as curves or surfaces) from functional samples evaluated at finitely many points. Two unique challenges arise in the functional context. Firstly, training data is often not evaluated along a fixed set of points. Secondly, steps must be taken to control the behaviour of the model between evaluation points, to mitigate overfitting. The proposed infinite-dimensional EBM employs a latent Gaussian process, which is weighted spectrally by an energy function parameterised with a neural network. The resulting EBM has the ability to utilize irregularly sampled training data and can output predictions at any resolution, providing an effective approach to up-scaling functional data. We demonstrate the efficacy of our proposed approach for modelling a range of datasets, including data collected from Standard and Poor's 500 (S&P) and UK National grid.

1 Introduction

The problem of generative modelling is concerned with learning distributions from samples. This challenge arises naturally in various applications of machine learning for which a number of well-established methods has been proposed including Variational Autoencoders [Kingma and Welling, 2013], Generative Adversarial Networks [Goodfellow et al., 2014] and Energy-Based Models (EBM) - which are intimately connected [Che et al., 2020].

Broadly, these methods all assume that the samples are intrinsically finite dimensional. When the underlying data is continuous, generative models are usually trained on a discretisation of the data, ultimately learning a probability distribution on a finite dimensional space whose dimension scales with the resolution of the data [Ramsay, 1982]. For example, in the context of images, the energy of an EBM is often defined on the same resolution of the data [Du and Mordatch, 2019].

In this work, we propose a novel class of generative model for data which is assumed to live within an infinite dimensional space of functions \mathcal{F} , which we assume to be a separable Hilbert space. In this setting, the data will consist of a finite set of function discretisations, each evaluated over a finite set of points. Based on this data, we seek to learn a generative model for the associated distribution over the function space \mathcal{F} directly. The functional data context poses unique challenges. Firstly, it is often the case that the evaluation points along which the functions are discretised is not uniform across samples, i.e., each function in the sample can be evaluated over a different set of points. We address this challenge by constructing a likelihood which can accommodate observations along irregular meshes. The second challenge relates to how to inform the characteristics of the learned functional distribution between evaluation points.

Generative models for functional data have been proposed in various contexts. One widely studied example is the Gaussian process (GP) and its higher dimensional generalisations. More specifically, a

Gaussian process $\mathcal{GP}(0, k)$ on the interval $[0, T]$ with kernel k can be associated to an infinite dimensional Gaussian measure $\mathcal{N}(0, \mathcal{C})$ supported on the space $L^2([0, T])$ of square integrable functions over $[0, T]$, with covariance operator $\mathcal{C}f = \int k(\cdot, y)f(y)dy$. While GPs are very flexible, they are not suitable for modelling distributions which exhibit multimodality or heteroskedasticity. To address this, various generalisations have been proposed which introduce nonlinear transformations to Gaussian processes to account for non-Gaussian behaviour (e.g., see Maroñas et al. [2021]). Recently, Mishra et al. [2020] proposed π -VAE, a method for encoding stochastic processes using variational autoencoders, as a means of developing an efficient prior for stochastic process models.

Our proposed methodology builds on the energy-based modelling (EBM) paradigm [Hinton, 2002], effectively providing a generalisation of EBMs to infinite dimensional spaces. In the classical setting, EBMs seek to learn a density proportional to $\exp(-E(x))$ over sample space. In this high-dimensional setting, the normalisation constant $Z = \int \exp(-E(x))dx$ (known as the partition function) is typically unknown and must be approximated. The energy function $E(\cdot)$, which is often parametrised using a neural network model, seeks to assign low-energy values to inputs x in the data distribution and high-energy values to others. Samples from a trained EBM are obtained implicitly, using Markov Chain Monte Carlo (MCMC) to sample from the unnormalised distribution. The flexibility and expressibility of the energy function give rise to several advantages of EBMs over other generative models such as those based on transformation of noise. One key advantage is its compositionality property that allows for incorporation of domain-specific knowledge through e.g. summing up two or more energy functions which represent different goals or constraints [Mnih and Hinton, 2005]. This fact makes EBMs promising candidates for modelling real life phenomena [Du et al., 2020, Matsubara et al., 2020] and thus have found applications in physics [Noé et al., 2019] and biology [Ingraham et al., 2019] to name a few. An application worth mentioning is the generation of synthetic data sets for instance in order to improve a classifier (SMOTE, see [Chawla et al., 2002]), improve image vison [Nikolenko, 2021] or to generate data sets with less privacy concerns.

An impediment in the deployment of EBMs on function space is the fact that there is no generalisation of the Lebesgue measure on an infinite-dimensional separable Hilbert space [Feldman, 1966]. This implies that there is no canonical reference measure on \mathcal{F} with respect to which a density of the form $\exp(-E(x))$ can be formulated. Instead, the proposed generative model is assumed to be absolutely continuous with respect to a probability measure \mathbb{P} associated to a Gaussian process taking values in \mathcal{F} . This measure effectively acts as a prior on \mathcal{F} , capturing intrinsic properties of the functional data such as regularity and integrability. This base measure \mathbb{P} can also be informed by data, either through hyper-parameter tuning or through preprocessing, as will be discussed in the later sections.

A key distinguishing feature between classical finite dimensional generative models and the proposed formulation is the ability to generate predictions along any mesh and at any resolution. This ability naturally leads to important applications, including up-scaling the resolution of functional data, as well as data imputation over irregularly sampled datasets. We demonstrate the efficacy of the proposed approach using both synthetic and real data-sets.

In summary, our contributions include:

- We introduce a novel class of energy-based models that is fully flexible and well adapted to functional data for density estimation and regression.
- We compare our proposed model with other popular models such as the Neural Process and Gaussian Process for density estimation and as well as function inference on a range of synthetic and real-life datasets.
- We demonstrate the benefits and abilities of our proposal for modelling FashionMNIST [Xiao et al., 2017] as a resolution independent model that can freely upscale and downscale images.

2 Background: Latent Energy Based Models

A common approach to generative modelling is to define an energy-based model (EBM) which captures the dependencies between variables by assigning a scalar value to a particular realisation of the variables. The function of the configuration of variables to a scalar (called the *energy* function $E_\theta : \mathcal{Y} \times \mathcal{Z} \rightarrow \mathbb{R}$) should assign low values to likely realisations and high values to unlikely realisations. The energy defines a model $p_\theta(Y, Z) = \frac{\exp(-E_\theta(Y, Z))}{C_\theta}$ where Y is observed, Z is a latent variable, and $C_\theta = \int_{\mathcal{Y}, \mathcal{Z}} \exp(-E_\theta(y, z))dydz$ is the normalising constant.

Given n samples from the data distribution $\mathbf{Y} := \{Y_i\}_{i=1}^n \stackrel{i.i.d.}{\sim} p(Y)$, the parameters of an EBM can be obtained by maximising an approximation to the marginal log-likelihood $\mathcal{L}(\theta) = \frac{1}{n} \sum_{i=1}^n \log \int_{\mathcal{Z}} p_{\theta}(Y_i, z) dz$ (known as Contrastive Divergence [Hinton, 2002]) whose derivative can be written as

$$\frac{\partial \mathcal{L}(\theta)}{\partial \theta} = \mathbb{E}_{Y_i \sim p(\mathbf{Y})} \mathbb{E}_{Z \sim p_{\theta}(Z|Y_i)} \left[\frac{\partial E_{\theta}(Y_i, Z)}{\partial \theta} \right] \quad (1)$$

$$- \mathbb{E}_{(Z, Y) \sim p_{\theta}(Z, Y)} \left[\frac{\partial E_{\theta}(Y, Z)}{\partial \theta} \right], \quad (2)$$

where $p(\mathbf{Y})$ is the empirical distribution of \mathbf{Y} . Intuitively, optimising Equation 1 results in a decrease of the energy of samples from the data distribution and increase in the synthetic samples which follows “analysis by synthesis” scheme [Grenander et al., 2007]. In general settings, Equation 1 is evaluated by estimating both the expectations from samples, and so we require a mechanism to generate samples generated from the conditional distribution $p_{\theta}(Z|Y)$ and joint distribution $p_{\theta}(Y, Z)$.

Generating samples from an EBM is itself a challenging problem. Common approaches of generating these samples is via a MCMC algorithm such as Hamiltonian Monte Carlo [Neal et al., 2011]. In our work, we utilise Langevin Monte Carlo without an accept/reject step [Neal, 1993, Section 5.3] with the following transition,

$$Y_{t+1} = Y_t - \frac{\lambda_t}{2} \nabla_{Y_t} E_{\theta}(Y_t, Z_t) + \sqrt{\lambda_t} \omega_t, \quad (3)$$

$$Z_{t+1} = Z_t - \frac{\lambda_t}{2} \nabla_{Z_t} E_{\theta}(Y_t, Z_t) + \sqrt{\lambda_t} \omega'_t, \quad (4)$$

where λ_t is the step size and $\omega_t, \omega'_t \sim \mathcal{N}(0, \mathbf{I})$. Samples from the conditional distribution $p_{\theta}(Z|Y)$ can be generated from utilising Equation 4 for a fixed Y_t . It can be shown that as $t \rightarrow \infty$ and $\lambda_t \rightarrow 0$ then we have $(Y_t, Z_t) \sim p_{\theta}(Y, Z)$ [Welling and Teh, 2011]. In practice, the chain is ran for a finite number of iterations with a fixed step size which is sufficient to produce samples close to its stationary distribution $p_{\theta}(Y, Z)$ [Teh et al., 2016, Vollmer et al., 2016].

3 Proposed Approach

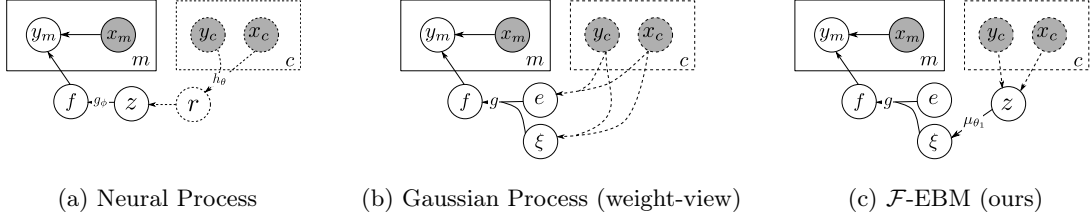


Figure 1: Graphical models of (a) Neural process, (b) Gaussian process, and (c) \mathcal{F} -EBM. Grey nodes indicate the variable is observed. Dashed lines indicate inference (given c context points). Continuous lines indicate the generative process, and dashed lines the inference.

Setting. We assume that we observe N independent realisations $f_1, \dots, f_N \in \mathcal{F}$ of an (unknown) probability measure \mathbb{P} supported on the space $\mathcal{F} : \mathcal{X} \rightarrow \mathcal{Y}$. For an arbitrary function f_i , it is evaluated on M (possibly distinct) points $X_i := (x_m)_{m=1}^M \subset \mathcal{X}^M$ taking values $Y_i := (f(x_m))_{m=1}^M \subset \mathcal{Y}^M$. In this setting, the dataset takes the form (\mathbf{X}, \mathbf{Y}) , where $\mathbf{X} = \{X_n\}_{n=1}^N$ and $\mathbf{Y} = \{Y_n\}_{n=1}^N$. Note that for notational simplicity, we shall assume that each representation has the same number of evaluation points. The extension to the more general setting is straightforward. Given the tuple (\mathbf{X}, \mathbf{Y}) , our objective is to learn a representation of the unknown probability distribution \mathbb{P} .

Gaussian Process (weight-view). Consider a mean-zero Gaussian process $\mathcal{GP}(0, k)$ with positive-definite kernel k . Through Mercer’s theorem, there exists an eigensystem $(\{\lambda_i\}_{i=1}^{\infty}, \{e_i(\cdot)\}_{i=1}^{\infty})$. In other words, we have $k(x, t) = \sum_{i=1}^{\infty} \lambda_i e_i(x) e_i(t)$ such that the eigenvalues λ_i and eigenfunctions $e_i(\cdot)$ are solutions to the eigenvalue problem $\lambda_i e_i(t) = \int_{\mathcal{X}} k(t, x) e_i(x) dx$. Realisations of the GP can be expressed as the following infinite sum (following from the Karhunen-Loeve expansion [Sullivan, 2015b, Section 11.1])

$$f(\cdot) = \sum_{i=1}^{\infty} \xi_i \sqrt{\lambda_i} e_i(\cdot), \quad (5)$$

where $\xi_i \sim \mathcal{N}(0, 1)$ is a sequence of independent random variables. Given $\xi = (\xi_i)_{i=1}^\infty$, we define a map $g(\xi)(\cdot) = \sum_i \xi_i \sqrt{\lambda_i} e_i(\cdot)$ such that $g(\xi) \sim \text{GP}(0, k)$ for $\xi \sim \Pi := \prod_{i=1}^\infty \mathcal{N}(0, 1)$. Figure 1b shows the graphical model of a GP in weight-space view.

Proposal: \mathcal{F} -EBM. The weight-view interpretation of a GP provides insights for defining a rich class of functions. Given a kernel and its (approximate) eigensystem $(\{\lambda_i\}_{i=1}^{d_\xi}, \{e_i(\cdot)\}_{i=1}^{d_\xi})$, we propose a distribution of functions which spectrally re-weights a GP using a learnt distribution. In other words, we have define a distribution of functions where each sample takes the form of $f(\cdot) = \sum_{i=1}^{d_\xi} \xi_i \sqrt{\lambda_i} e_i(\cdot)$, where $\xi := \mu_{\theta_1}(Z)$ is the transformation of the latent variable Z which has density proportional to $\exp(-\pi_{\theta_2}(Z))\Pi(Z)$, and where $\mu_{\theta_1} : \mathbb{R}^{d_Z} \rightarrow \mathbb{R}^{d_\xi}$ and $\pi_{\theta_2} : \mathbb{R}^{d_Z} \rightarrow \mathbb{R}$ are mappings which we parameterise with neural networks. Note that we truncate the infinite sum of Equation 5 to $d_\xi < \infty$ terms for tractability, and Π to $d_Z < \infty$ which can be thought of as the dimension of a latent variable. We will later show that this re-weighting results in a rich distribution of functions that can express complex and highly non-stationary datasets.

Given evaluations of a single function (X, Y) , we relate the observations to the underlying function using a likelihood function $L(Y; f, X)$. The likelihood is constructed by assuming that each point is sampled independently of each other. In order words, $L(Y; f, X)$ takes the form $\Pi_{i=1}^M \ell(y_i; f, x_i)$.

Combining the different components, we propose the following energy-based model:

$$p_\theta(Y, Z; X) \propto L(Y; g \circ \mu_{\theta_1}(Z), X) \exp(-\pi_{\theta_2}(Z))\Pi(Z),$$

where $\theta = (\theta_1, \theta_2)$ and whose graphical model can be seen in Figure 1c. The resulting probability measure is absolutely continuous with respect to the product measure $\Pi(Z)$. The model is trained by optimizing contrastive divergence (CD) [Hinton, 2002]. The computation of CD requires samples from the joint distribution $p_\theta(Y, Z; X)$ and the conditional distribution $p_\theta(Z | Y; X)$ which can be produced using Langevin MC. In Appendix A, we show that \mathcal{F} -EBM defines a valid stochastic process using Kolmogorov extension theorem and provide a summary of the theoretical properties of \mathcal{F} -EBM on infinite dimensional Hilbert spaces.

Estimating eigensystem of a kernel. For a given kernel k , we typically do not have analytical expressions for the associated Mercer eigensystem and must resort to numerical approximation. To this end, we employ the Nyström method to approximate the eigenvalue problem, i.e., we have

$$\lambda_i e_i(t) = \int_{\mathcal{X}} k(t, x) e_i(x) dp(x) \approx \frac{1}{l} \sum_{j=1}^l k(t, x_i) e_i(x_j), \quad (6)$$

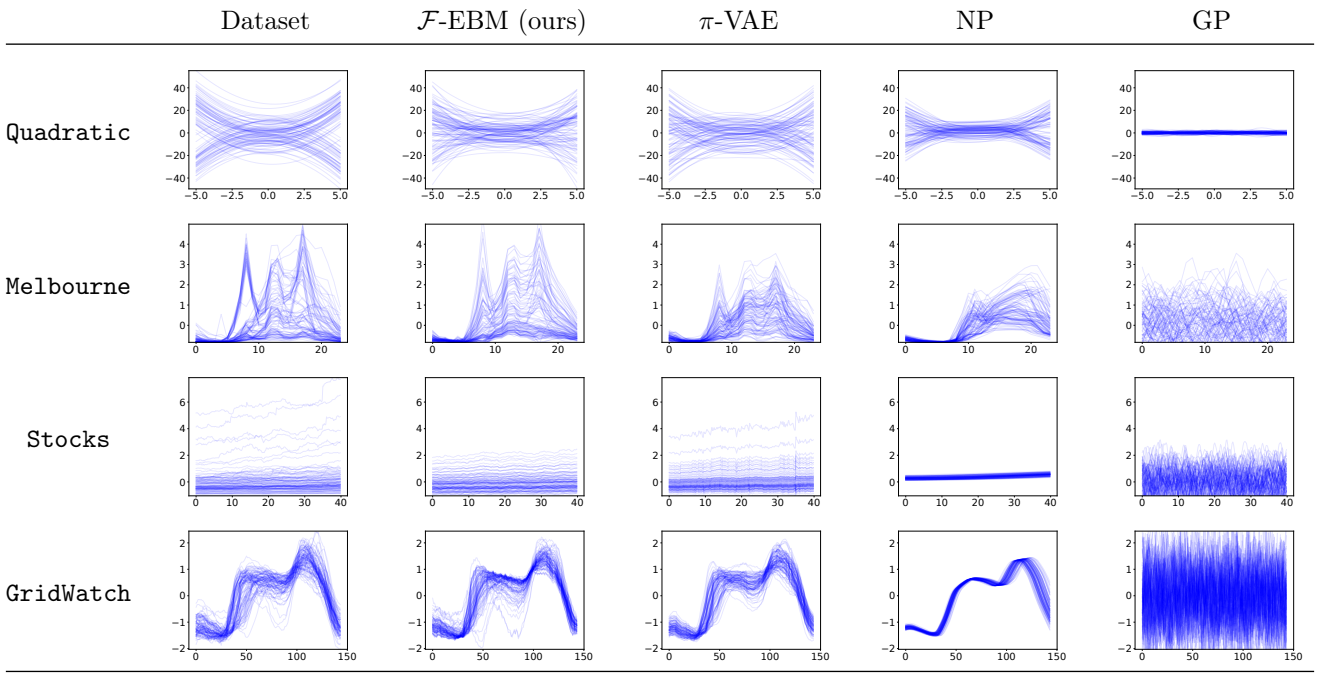
for some choice of $X := \{x_j\}_{j=1}^l \subset \mathcal{X}$ (see Baker [1979]). Substituting $t = x_k$ for $k = 1, \dots, l$ results in an eigenvalue problem $\frac{1}{l} K(X, X) \hat{e}_i(X) = \hat{\lambda}_i \hat{e}_i(X)$ where $K(X, X) = (k(x_i, x_j)_{ij}) \in \mathbb{R}^{l \times l}$ is the gram matrix, and $\hat{e}_i(X) = [\hat{e}_i(x_1), \dots, \hat{e}_i(x_l)]^\top \in \mathbb{R}^l$. Solving for the eigenspectrum of scaled gram matrix $\frac{1}{l} K(X, X)$ yields estimates of l non-negative eigenvalues¹. The eigenvectors correspond to the eigenfunctions $\{\hat{e}_i\}^l$ evaluated at X . We require the eigenfunctions to be evaluated at arbitrary locations. One method is plugging the estimates back into Equation 6 [Williams and Seeger, 2001]. However, we found that the estimates of eigenfunctions with small eigenvalues were not accurate, and so kernel ridge regression was used instead.

Inference of f . Given a context pair (X^c, Y^c) , one may want to infer the underlying latent function f . To do this, we first obtain samples from the conditional distribution $p(Z | Y; X)$, which is then passed through the map μ_θ to induce a distribution over the weights of the eigenfunctions. Then, the map g can be used to transform the weights into functions (see Figure 1c). We write $p(f | Y; X)$ to denote the distribution of $g \circ \mu_{\theta_1}(Z) | Y; X$. Inference of a function (corresponding to a potentially infinite-dimensional vector) is cast as inference of Z with a much lower dimensionality and allows for efficient use of MCMC methods.

Kernel Choice. The kernel can be used to capture any prior belief about the underlying function and plays a crucial role in the learnt model. One method is to construct kernels from the product and sums of well-studied existing kernels such as the Gaussian and Matérn kernel [Rasmussen and Williams, 2006, see Section 4.2]. Other choices include constructing an explicit feature map with a neural network, or obtain a data-driven basis via functional Principal component analysis. A combination of all the aforementioned methods can be also used in conjunction.

¹The estimates $\hat{\lambda}_i$ which converge to λ_i in the limit $l \rightarrow \infty$ [Baker, 1979, Theorem 3.4].

Table 1: Visualisation of 100 samples drawn from the dataset, \mathcal{F} -EBM (ours), π -VAE, Neural Process (NP), and Gaussian Process (GP).



4 Related Work

Stochastic processes provide an elegant method for defining distributions of functions. A popular example is the Gaussian processes (GP) [Rasmussen and Williams, 2006]. More recently, neural processes (NP) and its variants [Garnelo et al., 2018a,b] has been proposed to learn an approximation of a stochastic process by combining the perks of GPs and neural networks for scalable inference while quantifying its uncertainty. While GPs and NPs can be used as generative models, the focus has been on uncertainty quantification and prediction rather than generative modelling. The form of NP is similar to the VAE [Kingma and Welling, 2013]. The recently proposed π -VAE [Mishra et al., 2020] extends the VAE formalism to function classes, effectively providing a generative model for stochastic processes. This is achieved by performing a decomposition of the data onto a finite basis of functions. The encoder/decoder pair are then trained to learn the distribution of the associated basis coefficients, from which realisations of the learned stochastic process can be readily generated.

There are other related works that focuses on learning implicit representations of images as functions [Dupont et al., 2021, Anokhin et al., 2021] and physics-informed modelling [Yang et al., 2020, Meng et al., 2021]. Dupont et al. [2021] proposed a GAN approach for learning a generative model for images as functions. Distinctly from the approach proposed here, their model does not learn the underlying functional distribution associated to the data. Concurrently, PI-GAN [Yang et al., 2020] proposed as a GAN approach for learning an approximation of a stochastic process, focusing on endowing the generator with prior knowledge in the form of stochastic differential equation. Meng et al. [2021] extended it further by using DeepONets [Lu et al., 2019] to incorporate physical knowledge and proposed a method for inference of the latent function by using HMC [Neal et al., 2011]. Note that the form of the PI-GAN requires some extensions to accommodate for learning functions with different evaluation points whilst our proposal does not.

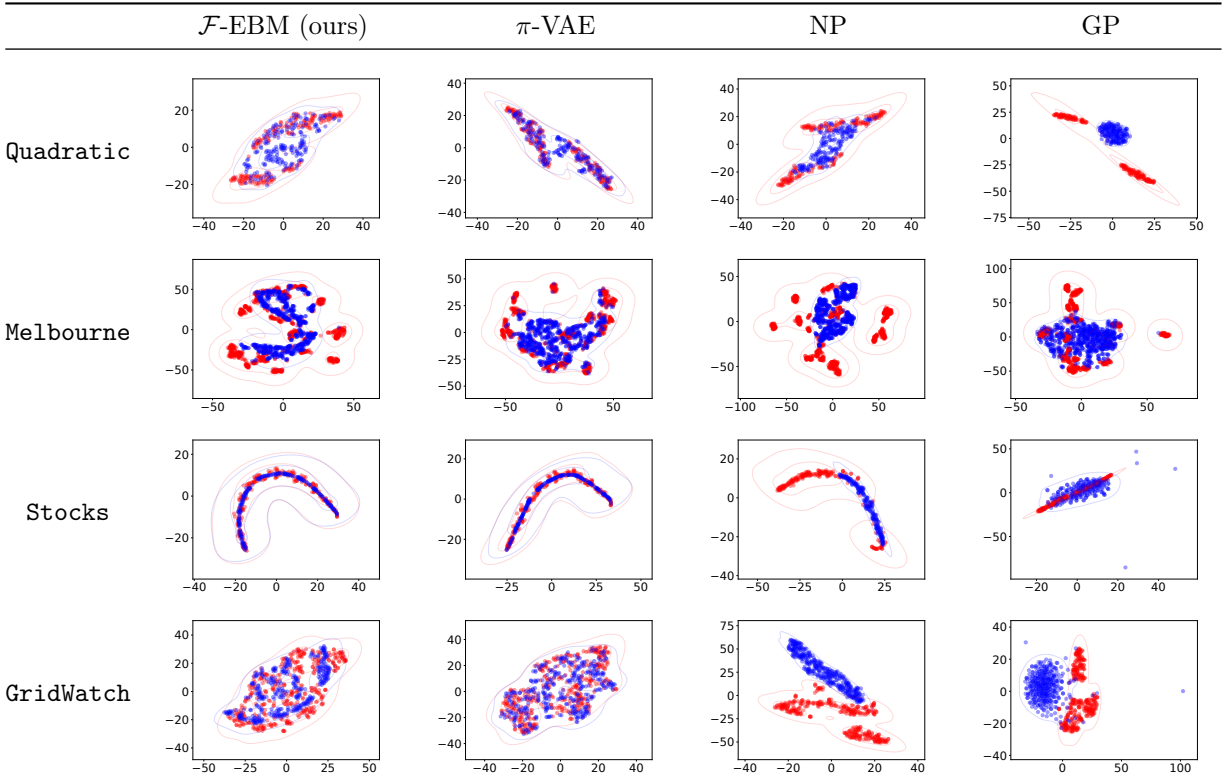
5 Experiments

In Section 5.1, we benchmark our model against existing models such as π -VAE, GP, and NP on synthetic and real data. Then in Section 5.1, we show how our proposal can be used as a resolution-independent generative model that can freely upscale and downscale images. The details for the experiments can be found in the Appendix B. The code will be made available after the review period.

5.1 Benchmark

We utilize four datasets composed of one synthetic and three real-world datasets. The samples from the dataset can be seen in Table 1. The first **Quadratic** ($n = 400, m = 30$) is a bi-modal dataset composed of quadratic functions that was generated by sampling the sign of the quadratic term from a uniform distribution on $\{-1, 1\}$. The dataset was designed to test the model’s capacity to express bi-modality. We use 200 samples for training and the remainder for evaluation. The second **Melbourne** ($n = 1138, m = 24$) is a real-life dataset where each sample is the number of pedestrians on a certain street in Melbourne recorded throughout different times of the day. We use 796 samples for training and the remainder for evaluation. The third dataset **GridWatch** ($n = 532, m = 144$) is another real-life dataset where each sample is the demand of energy on the UK National Grid throughout different times of the day. We use 372 samples for training and the remainder for evaluation. Finally, we use **Stocks** ($n = 400, m = 200$) where each sample corresponds to a stock highest performance on that day, recorded over 200 days starting from February 2013 (when data is available). The data is taken from S&P 500. We use 200 samples for training and the remainder for evaluation. See Appendix B.3 for preprocessing details. These datasets are “simple”, in the sense, that they are low dimensional, but they exhibit complex properties such as bimodality, multi-modality and large support. For these datasets, we choose $\ell(\cdot|\cdot)$ to be the Gaussian likelihood.

Table 2: The t-SNE embeddings of 100 samples of both samples generated from the model (blue) and samples from the data (red).



Evaluation. We measure the quality of the trained model by considering its *goodness-of-fit* and *predictive error*. We compare our proposed model to a Gaussian process (GP) implemented in GPyTorch [Gardner et al., 2018], a Neural process (NP) which follows recommended practices [Le et al., 2018], and our own implementation of π -VAE (see Section 4).

Goodness-of-fit. It is desirable for our model to be a good fit to the data distribution. Since evaluating generative models is highly difficult, we consider three methods for evaluating the fit: (1) we visually inspect the samples generated from the model; (2) following Yoon et al. [2019], we visually evaluate this by plotting a 2-dimensional embeddings of both the samples generated by the model and taken from the dataset. A high degree of overlap between the data and model embedding’s distribution suggests a good fit to the data distribution. We apply dimensionality reduction methods (such as t-SNE [Van der Maaten and Hinton, 2008] and PCA [Bryant and Yarnold, 1995]) on both the original data and the generated

synthetic samples; (3) as a quantitative measure, we evaluate the model’s fit by computing the test power of a functional non-parametric two-sample test to compare the synthetic samples and samples from the dataset. Since all models are wrong [Box, 1976], we expect the test to reject the null hypothesis that the learnt model is equal to the generating process of the dataset and so, the test power will indicate the fidelity of the model. We use the test proposed by Wynne and Duncan [2020].

Table 3: Test power of two-sample test comparing samples of the data with samples from the model. **Bold** indicates the best score (lower is better). The test power is averaged over 200 trials with 10 samples drawn from the dataset and model at significance level $\alpha = 0.05$.

	Dataset			
	Polynomial	Melbourne	Stocks	GridWatch
\mathcal{F} -EBM (ours)	0.19 ± 0.04	0.09 ± 0.03	0.08 ± 0.03	0.09 ± 0.03
π -VAE	0.22 ± 0.06	0.32 ± 0.04	0.11 ± 0.03	0.16 ± 0.04
Neural Process	0.59 ± 0.06	0.95 ± 0.02	1.00 ± 0.00	1.00 ± 0.00
Gaussian Process	1.00 ± 0.00	0.77 ± 0.05	0.67 ± 0.04	1.00 ± 0.00

Predictive error. The predictive distribution is one of the central quantities of interest for NPs and GPs. We measure its fidelity with the difference between the mean function of the model and the underlying “true” function. Since the underlying function is usually unknown to us (except in synthetic settings), we split the dataset into disjoint sets where one will be used to infer the function and the other is used to evaluate the conditional distribution. Given a portion $p \in (0, 1)$, we consider three methods for splitting the dataset (X, Y) to create the context pair (X^c, Y^c) and the evaluation pair (X^e, Y^e) such that the context pair has p portion of the original data (and $1 - p$ for the evaluation dataset). As shown in Figure 2, the splits were chosen either (a) uniformly without replacement, (b) selected to be between sampled points in the infer dataset, or (c) down-sampled version of the original sampled points. We report the mean of squared errors averaged over the evaluation set., i.e, $\mathbb{E}_{\text{data}} \left[\frac{1}{n \lceil (1-p) \rceil} \sum_{(x_i, y_i) \in (X^e, Y^e)} (\mathbb{E}[f(x_i)] - y_i)^2 \right]$ where the inner expectation is estimated using samples from $p(f \mid Y^c; X^c)$.

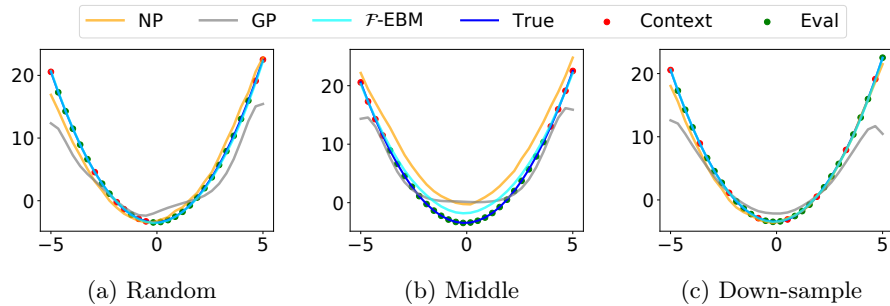


Figure 2: A visualisation of the three methods used for splitting evaluations (X, Y) of a quadratic function with $p = \frac{1}{4}$. The context pair (X^c, Y^c) shown in red used to compute the mean function for various models (\mathcal{F} -EBM, GP and NP) which is evaluated on the evaluation pair (X^e, Y^e) shown in green.

Goodness-of-fit. Table 1 shows samples generated from the model and samples from the dataset. Since NP and GP were designed with regression in mind, it is unsurprising that both \mathcal{F} -EBM and π -VAE can capture the intricacies of the dataset better than both the NP and GP. For the GP, it is clear that it cannot capture the datasets effectively due to its stationary kernel. As for the NP, the model can capture certain characteristics of the dataset (such as the mode) but cannot capture the tails of the data distribution. These results can be visually verified further in the Table 2 which shows the t-SNE embeddings for each model against its respective datasets. The table highlights a high degree of overlap for \mathcal{F} -EBM and π -VAE compared to the other models (see Appendix Table 5 for PCA embeddings). It is hard to distinguish between π -VAE and \mathcal{F} -EBM using only samples and its embeddings. However, the results of the test power of the two-sample test shown in Table 3 tells a different story. It can be seen that \mathcal{F} -EBM achieves the lowest test power with π -VAE being a close contender. These results suggest that \mathcal{F} -EBM is a good choice for density estimation.

Predictive Error. Table 4 shows the prediction error on a range of datasets. Both NP and GP are

Table 4: The mean of squared errors to measure the mismatch between the mean function and the true function on unseen points. The mean function is averaged from 100 samples drawn from $p(f | X^c, Y^c)$. The error is computed on the evaluation pair and averaged over the evaluation dataset. **Bold** indicates the lowest score (lower is better). High indicates a value greater than 100.

Dataset	Model	Downsample			Middle			Random		
		$p = \frac{1}{4}$	$p = \frac{1}{3}$	$p = \frac{1}{2}$	$p = \frac{1}{4}$	$p = \frac{1}{2}$	$p = \frac{3}{4}$	$p = \frac{1}{4}$	$p = \frac{1}{2}$	$p = \frac{3}{4}$
Quadratic	\mathcal{F} -EBM	0.034	0.033	0.016	1.802	0.045	0.010	0.041	0.011	0.007
	π -VAE	0.144	0.167	0.092	High	7.402	0.025	1.001	0.330	0.027
	NP	7.431	10.491	9.447	34.785	15.596	3.112	8.048	7.686	7.599
	GP	28.089	36.523	19.934	High	75.350	25.556	70.742	39.231	8.275
Melbourne	\mathcal{F} -EBM	0.217	0.303	0.164	0.865	0.591	0.230	0.398	0.323	0.230
	π -VAE	High	0.393	0.195	High	32.294	0.082	12.288	0.860	0.093
	NP	0.194	0.179	0.174	1.271	1.016	0.452	0.231	0.278	0.266
	GP	0.424	0.420	0.213	1.526	1.450	0.723	1.047	0.648	0.508
Stocks	\mathcal{F} -EBM	0.022	0.019	0.017	0.022	0.013	0.006	0.023	0.017	0.016
	π -VAE	0.030	0.030	0.022	High	High	High	High	0.023	0.011
	NP	0.039	0.037	0.037	0.092	0.040	0.018	0.038	0.039	0.041
	GP	0.053	0.031	0.017	1.133	1.081	0.938	0.135	0.036	0.011
GridWatch	\mathcal{F} -EBM	0.069	0.058	0.045	0.103	0.092	0.051	0.080	0.049	0.038
	π -VAE	0.376	0.330	0.249	High	High	High	High	0.260	0.122
	NP	0.158	0.155	0.160	0.162	0.178	0.123	0.163	0.166	0.159
	GP	0.338	0.209	0.106	0.938	0.581	0.389	0.567	0.283	0.156

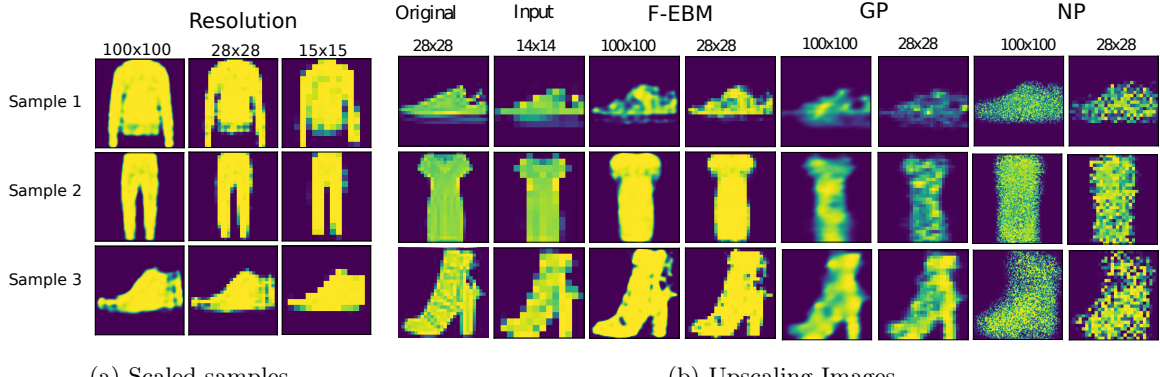


Figure 3: Visualization of synthetic samples learnt from FashionMNIST. Figure 3a shows the three functions evaluated at different resolutions. Figure 3b displays upsampled samples generated by \mathcal{F} -EBM, GP and NP conditioned on the “Input” which is a downsampled variant the “Original” image.

designed for regression, and are competitive baselines for this problem. However, the performance of GP on **Quadratic** is noticeably poorer than others. This may be due to us not performing any pre-processing for **Quadratic**. For the GP, interpolating between regions where there are not many observe points the mean will tend towards the prior mean which will accumulate large errors in this problem (see Figure 2) due to the fact the learnt kernel is simple and unable to learn the data distribution. For other datasets where we pre-process the dataset, GP produces more competitive results. π -VAE also has high errors particularly on the “Middle” split and small context pair on “Random”. This is due to error from estimating the initial coefficients for small context pairs which leads to high errors in the approximate posterior distribution. NPs performs well on all datasets and affirms that NP is a good choice for regression. Overall, it can be seen that \mathcal{F} -EBM performs competitively across all datasets.

5.2 Resolution-independent learning of images

One of the benefits of \mathcal{F} -EBM is its ability to learn complex kernels. We demonstrate this on a complex regression task of predicting the pixel value for an entire image. In this setting, the inputs corresponds to the random fourier feature embedding [Tancik et al., 2020] of the Cartesian coordinate of each pixel and the output is the pixel intensity. We train our model on FashionMNIST dataset [Xiao et al., 2017]. Since Y is pixel data defined on $[0, 1]$, we define the likelihood $\ell(\cdot | \cdot)$ to the continuous Bernoulli [Loaiza-Ganem and Cunningham, 2019].

It can be seen that in Figure 4 that the model can produce diverse samples for shoes, shirts, and others. Unlike most generative models, our proposed approach can scale the images to arbitrary resolutions, as can be seen in Figure 3a and 3b. In Figure 3a, we demonstrate for each sample the model can upscale (or downscale) beyond the dataset’s resolution. This is because each sample is a function that can be evaluated at any scale we desire. Figure 3b shows a sampled function from the model conditioned on a downsampled input from the dataset. The model can accurately infer the underlying function which can be used to produce high (or low) resolution images. For completeness, we also show conditional samples for GP and NP.

6 Conclusion, Limitations and Future work

We introduced \mathcal{F} -EBM, a class of models that are suitable for learning functional data distributions. We have shown that \mathcal{F} -EBM can accurately perform inference over function space, which performs similarly or better than current approaches.

The most important limitations of our proposed work pertains to the choice of hyperparameters such as the kernel of the reference measure, truncation dimensions and architecture of the neural network. Although there is a large range of possible choices, we would like to emphasise that we did not perform a significant amount of hyperparameter tuning between problems and note that we used the Matérn kernel, and two-layered neural network for all our problems. Mitigating these issues and finding a method for choosing these hyperparameters are left for future work.

Whilst its performance is strong, it is computationally more expensive than other methods. The main computational burden lies in the use of Contrastive divergence which requires us to run long MCMC chains to compute the loss function. We found that there are still gains to be had by tuning the CD algorithm and so, improving the CD algorithm itself could be a fruitful line of future work. On the other hand, there are other methods for training unnormalised distribution (such as score matching methods [Hyvärinen and Dayan, 2005]) that can also be considered.

An extension can be made to \mathcal{F} -EBM to perform conditional density estimation by simply encoding an additional variable as input to the neural network. This extension will allow the model to learn on conditional distributions that will be independent of the resolution of the data, which is usually what is being considered in current models (see conditional GANs [Mirza and Osindero, 2014] for instance).

References

- I. Anokhin, K. Demochkin, T. Khakhulin, G. Sterkin, V. Lempitsky, and D. Korzhenkov. Image generators with conditionally-independent pixel synthesis. In *Proceedings of the IEEE/CVF Conference on Computer Vision and Pattern Recognition*, pages 14278–14287, 2021.
- C. T. H. Baker. *Numerical Integration in the Treatment of Integral Equations*, pages 44–53. Birkhäuser Basel, Basel, 1979. ISBN 978-3-0348-6288-2. doi: 10.1007/978-3-0348-6288-2_2. URL https://doi.org/10.1007/978-3-0348-6288-2_2.
- G. E. Box. Science and statistics. *Journal of the American Statistical Association*, 71(356):791–799, 1976.
- F. B. Bryant and P. R. Yarnold. Principal-components analysis and exploratory and confirmatory factor analysis. 1995.
- N. V. Chawla, K. W. Bowyer, L. O. Hall, and W. P. Kegelmeyer. SMOTE: Synthetic minority over-sampling technique. *J. Artif. Intell. Res.*, 16:321–357, June 2002.
- T. Che, R. Zhang, J. Sohl-Dickstein, H. Larochelle, L. Paull, Y. Cao, and Y. Bengio. Your GAN is secretly an energy-based model and you should use discriminator driven latent sampling. Mar. 2020.
- Y. Du and I. Mordatch. Implicit generation and modeling with energy based models. In H. Wallach, H. Larochelle, A. Beygelzimer, F. d'Alché-Buc, E. Fox, and R. Garnett, editors, *Advances in Neural Information Processing Systems*, volume 32. Curran Associates, Inc., 2019. URL <https://proceedings.neurips.cc/paper/2019/file/378a063b8fdb1db941e34f4bde584c7d-Paper.pdf>.
- Y. Du, J. Meier, J. Ma, R. Fergus, and A. Rives. Energy-based models for atomic-resolution protein conformations. In *International Conference on Learning Representations*, 2020. URL https://openreview.net/forum?id=S1e_9xrFvS.
- E. Dupont, Y. W. Teh, and A. Doucet. Generative models as distributions of functions. *arXiv preprint arXiv:2102.04776*, 2021.
- S. Elfwing, E. Uchibe, and K. Doya. Sigmoid-weighted linear units for neural network function approximation in reinforcement learning. *Neural Networks*, 107:3–11, 2018.
- J. Feldman. Nonexistence of quasi-invariant measures on infinite-dimensional linear spaces. *Proceedings of the American Mathematical Society*, 17(1):142–146, 1966.
- J. R. Gardner, G. Pleiss, D. Bindel, K. Q. Weinberger, and A. G. Wilson. Gpytorch: Blackbox matrix-matrix gaussian process inference with gpu acceleration. In *Advances in Neural Information Processing Systems*, 2018.
- M. Garnelo, D. Rosenbaum, C. Maddison, T. Ramalho, D. Saxton, M. Shanahan, Y. W. Teh, D. Rezende, and S. A. Eslami. Conditional neural processes. In *International Conference on Machine Learning*, pages 1704–1713. PMLR, 2018a.
- M. Garnelo, J. Schwarz, D. Rosenbaum, F. Viola, D. J. Rezende, S. Eslami, and Y. W. Teh. Neural processes. *arXiv preprint arXiv:1807.01622*, 2018b.
- I. J. Goodfellow, J. Pouget-Abadie, M. Mirza, B. Xu, D. Warde-Farley, S. Ozair, A. Courville, and Y. Bengio. Generative adversarial nets. In *Proceedings of the 27th International Conference on Neural Information Processing Systems - Volume 2*, NIPS'14, page 2672–2680, Cambridge, MA, USA, 2014. MIT Press.
- U. Grenander, M. I. Miller, M. Miller, et al. *Pattern theory: from representation to inference*. Oxford university press, 2007.
- G. E. Hinton. Training products of experts by minimizing contrastive divergence. *Neural computation*, 14(8):1771–1800, 2002.
- A. Hyvärinen and P. Dayan. Estimation of non-normalized statistical models by score matching. *Journal of Machine Learning Research*, 6(4), 2005.

- J. Ingraham, A. J. Riesselman, C. Sander, and D. S. Marks. Learning protein structure with a differentiable simulator. In *ICLR*, 2019.
- D. P. Kingma and M. Welling. Auto-encoding variational bayes. *arXiv preprint arXiv:1312.6114*, 2013.
- T. A. Le, H. Kim, M. Garnelo, D. Rosenbaum, J. Schwarz, and Y. W. Teh. Empirical evaluation of neural process objectives. In *NeurIPS workshop on Bayesian Deep Learning*, 2018.
- G. Loaiza-Ganem and J. P. Cunningham. The continuous bernoulli: fixing a pervasive error in variational autoencoders. In H. Wallach, H. Larochelle, A. Beygelzimer, F. d'Alché-Buc, E. Fox, and R. Garnett, editors, *Advances in Neural Information Processing Systems*, volume 32. Curran Associates, Inc., 2019. URL <https://proceedings.neurips.cc/paper/2019/file/f82798ec8909d23e55679ee26bb26437-Paper.pdf>.
- L. Lu, P. Jin, and G. E. Karniadakis. Deeponet: Learning nonlinear operators for identifying differential equations based on the universal approximation theorem of operators. *arXiv preprint arXiv:1910.03193*, 2019.
- J. Maroñas, O. Hamelijnck, J. Knoblauch, and T. Damoulas. Transforming gaussian processes with normalizing flows. In *International Conference on Artificial Intelligence and Statistics*, pages 1081–1089. PMLR, 2021.
- T. Matsubara, A. Ishikawa, and T. Yaguchi. Deep energy-based modeling of discrete-time physics. *Advances in Neural Information Processing Systems*, 33, 2020.
- X. Meng, L. Yang, Z. Mao, J. d. A. Ferrandis, and G. E. Karniadakis. Learning functional priors and posteriors from data and physics. *arXiv preprint arXiv:2106.05863*, 2021.
- M. Mirza and S. Osindero. Conditional generative adversarial nets. *arXiv preprint arXiv:1411.1784*, 2014.
- S. Mishra, S. Flaxman, H. Zhu, and S. Bhatt. π vae: Encoding stochastic process priors with variational autoencoders. *arXiv preprint arXiv:2002.06873*, 2020.
- A. Mnih and G. Hinton. Learning nonlinear constraints with contrastive backpropagation. In *Proceedings. 2005 IEEE International Joint Conference on Neural Networks, 2005.*, volume 2, pages 1302–1307. IEEE, 2005.
- R. M. Neal. *Probabilistic inference using Markov chain Monte Carlo methods*. Department of Computer Science, University of Toronto Toronto, ON, Canada, 1993.
- R. M. Neal et al. Mcmc using hamiltonian dynamics. *Handbook of markov chain monte carlo*, 2(11):2, 2011.
- S. I. Nikolenko. *Synthetic Data for Basic Computer Vision Problems*, pages 161–194. Springer International Publishing, Cham, 2021. ISBN 978-3-030-75178-4. doi: 10.1007/978-3-030-75178-4_6. URL https://doi.org/10.1007/978-3-030-75178-4_6.
- F. Noé, S. Olsson, J. Köhler, and H. Wu. Boltzmann generators: Sampling equilibrium states of many-body systems with deep learning. *Science*, 365(6457), 2019.
- G. D. Prato. *An Introduction to Infinite-Dimensional Analysis*. Springer Berlin Heidelberg, 2006. doi: 10.1007/3-540-29021-4. URL <https://doi.org/10.1007/3-540-29021-4>.
- J. Ramsay. When the data are functions. *Psychometrika*, 47(4):379–396, 1982.
- C. Rasmussen and C. Williams. Gaussian processes for machine learning. gaussian processes for machine learning, 2006.
- T. Sullivan. *Introduction to Uncertainty Quantification*. Springer International Publishing, 2015a. doi: 10.1007/978-3-319-23395-6. URL <https://doi.org/10.1007/978-3-319-23395-6>.
- T. J. Sullivan. *Introduction to uncertainty quantification*, volume 63. Springer, 2015b.
- M. Tancik, P. P. Srinivasan, B. Mildenhall, S. Fridovich-Keil, N. Raghavan, U. Singhal, R. Ramamoorthi, J. T. Barron, and R. Ng. Fourier features let networks learn high frequency functions in low dimensional domains. *NeurIPS*, 2020.

- Y. W. Teh, A. H. Thiery, and S. J. Vollmer. Consistency and fluctuations for stochastic gradient langevin dynamics. *J. Mach. Learn. Res.*, 17(1):193–225, Jan. 2016.
- L. Van der Maaten and G. Hinton. Visualizing data using t-sne. *Journal of machine learning research*, 9(11), 2008.
- S. J. Vollmer, K. C. Zygalakis, and Y. W. Teh. Exploration of the (non-)asymptotic bias and variance of stochastic gradient langevin dynamics. *J. Mach. Learn. Res.*, 17(1):5504–5548, Jan. 2016.
- M. Welling and Y. W. Teh. Bayesian learning via stochastic gradient langevin dynamics. In *Proceedings of the 28th international conference on machine learning (ICML-11)*, pages 681–688. Citeseer, 2011.
- C. Williams and M. Seeger. Using the nyström method to speed up kernel machines. In *Proceedings of the 14th annual conference on neural information processing systems*, number CONF, pages 682–688, 2001.
- G. Wynne and A. B. Duncan. A kernel two-sample test for functional data. *arXiv preprint arXiv:2008.11095*, 2020.
- H. Xiao, K. Rasul, and R. Vollgraf. Fashion-mnist: a novel image dataset for benchmarking machine learning algorithms, 2017.
- L. Yang, D. Zhang, and G. E. Karniadakis. Physics-informed generative adversarial networks for stochastic differential equations. *SIAM Journal on Scientific Computing*, 42(1):A292–A317, 2020.
- J. Yoon, D. Jarrett, and M. van der Schaar. Time-series generative adversarial networks. In H. Wallach, H. Larochelle, A. Beygelzimer, F. d'Alché-Buc, E. Fox, and R. Garnett, editors, *Advances in Neural Information Processing Systems*, volume 32. Curran Associates, Inc., 2019. URL <https://proceedings.neurips.cc/paper/2019/file/c9efe5f26cd17ba6216bbe2a7d26d490-Paper.pdf>.

\mathcal{F} -EBM: Energy Based Learning of Functional Data

Supplementary

A Mathematical Background

In this section we provide some background on the mathematical formulation of stochastic processes as random variables on Hilbert spaces. An important class of stochastic process which are central to this work is the Gaussian process [Rasmussen and Williams, 2006]. Let $\mathcal{D} \subset \mathbb{R}^d$ be compact. Given a positive definite kernel $k : \mathcal{D} \times \mathcal{D} \rightarrow \mathbb{R}$ and a function $m : \mathcal{D} \rightarrow \mathbb{R}$ we say x is a Gaussian process with mean function m and covariance function k if for every finite collection of points $\{s_n\}_{n=1}^N$ the random vector $(x(s_1), \dots, x(s_N))$ is a multivariate Gaussian random variable with mean vector $(m(s_1), \dots, m(s_N))$ and covariance matrix $k(s_n, s_m)_{n,m=1}^N$. The mean function and covariance function completely determines the Gaussian process. We write $x \sim \mathcal{GP}(m, k)$ to denote the Gaussian process with mean function m and covariance function k .

Let X be a real, separable Hilbert space with inner product $\langle \cdot, \cdot \rangle$ and norm $\|\cdot\|$. Let $\mathcal{B}(X)$ be the Borel σ -algebra on X . A measure μ on $X, \mathcal{B}(X)$ is said to be Gaussian if there exists $m \in X$ and a linear operator C such that the push-forward $l_h_*\mu$ is a Gaussian measure on $(\mathbb{R}, \mathcal{B}(\mathbb{R}))$ with mean $\langle h, m \rangle$ and variance $\langle h, Ch \rangle$, for all $h \in H$ where $l_h(\cdot) = \langle h, \cdot \rangle$. The element $m \in X$ is called the *mean* and C is the covariance operator, which is a symmetric non-negative operator with finite trace. The characteristic functional of a Gaussian measure μ on X satisfies

$$\widehat{\mu}(\lambda) = \int_X e^{i\langle \lambda, x \rangle} \mu(dx) = e^{i\langle m, \lambda \rangle - \frac{1}{2}\langle Ch, \lambda \rangle}.$$

It is therefore uniquely determined by m and C . We therefore use the notation $\mu \equiv N_{m,C}$. See [Prato, 2006] for further properties of Gaussian measures on Hilbert spaces.

Gaussian processes can be uniquely associated to a Gaussian measures on the $X = L^2(\mathcal{D})$. Indeed, a Gaussian process $\mathcal{GP}(m, k)$ on \mathcal{D} , where $m \in L^2(\mathcal{D})$ and k is positive-definite continuous, is characterised by a Gaussian measure on X with mean m and covariance operator defined by

$$Cf(\cdot) = \int k(\cdot, y) f(y) dy, \quad \forall f \in L^2(\mathcal{D}).$$

It can be shown that the covariance C is a positive trace class operator which admitting the spectral decomposition $C = \sum_{i=1}^{\infty} \lambda_i e_i \langle e_i, \cdot \rangle$, where $\{\{\lambda_i\}_{i=1}^{\infty}, \{e_i\}_{i=1}^{\infty}\}$ is the eigensystem associated with the operator C . Moreover we can write the kernel as $k(x, y) = \sum_{i=1}^{\infty} \lambda_i e_i(x) e_i(y)$, for all $x, y \in \mathcal{D}$.

Given a second-order stochastic process $x(\cdot)$ taking values in $L^2(\mathcal{D})$ the Karhunen-Loeve expansion provides an important characterisation. Suppose that the point-wise covariance $k(s, t) = \text{Cov}[x(s), x(t)]$ is continuous and the mean function defined by $t \rightarrow m(t) = \mathbb{E}[x(t)]$ lies in $L^2(\mathcal{D})$. Let C be the non-negative definite trace class covariance operator associated to k , and let $\{\{\lambda_i\}_{i=1}^{\infty}, \{e_i\}_{i=1}^{\infty}\}$ eigensystem. The Karhunen-Loeve expansion [Sullivan, 2015a, Theorem 11.4] for the random process $x(\cdot)$ is given by

$$x(\cdot) \sim m + \sum_{i=1}^{\infty} \sqrt{\lambda_i} \xi_i e_i(\cdot),$$

where $\{\xi_i\}_{i=1}^{\infty}$ are unit-variance uncorrelated random variables. In special case where the process $x(\cdot)$ is Gaussian then the ξ_i are actually independent standard Gaussian random variables, yielding a convenient means of generating realisations of the process, when the eigensystem of the covariance is available.

The model proposed in Section 3 is characterised by the density of the joint distribution of $Y = (f(x_1), \dots, f(x_M))$, for a set of evaluation points $X = (x_1, \dots, x_M)$ in \mathcal{X} defined by

$$\begin{aligned} p(y_1, \dots, y_M | x_1, \dots, x_M) &\propto \int L(Y, g \circ \mu_{\theta}(z); X) \exp(-\pi_{\theta'}(z)) \Pi(dz) \\ &= \int \prod_{i=1}^M l(y_i | x_i, g \circ \mu_{\theta}(z)) \exp(-\pi_{\theta'}(z)) \Pi(dz). \end{aligned}$$

To show that this characterises a stochastic process indexed by \mathcal{X} we verify Kolmogorov's consistency conditions. Firstly note that, for any permutation π_1, \dots, π_M of $1, \dots, M$, then

$$\begin{aligned} p(y_{\pi_1}, \dots, y_{\pi_M} | x_{\pi_1}, \dots, x_{\pi_M}) &= \frac{1}{Z} \int \prod_{i=1}^M l(y_{\pi_i} | x_{\pi_i}, g \circ \mu_\theta(z)) \exp(-\pi_{\theta'}(z)) \Pi(dz), \\ &= \frac{1}{Z} \int \prod_i^M l(y_i | x_i, g \circ \mu_\theta(z)) \exp(-\pi_{\theta'}(z)) \Pi(dz) \\ &= p(y_1, \dots, y_M | x_1, \dots, x_M), \end{aligned}$$

where $Z = \int \dots \int \prod_{i=1}^M l(y_i | x_i, g \circ \mu_\theta(z)) \Pi(dz) dy_1 \dots dy_M$. Secondly, we show that the finite dimensional distributions are consistent with respect to marginalisation. To this end, consider

$$\begin{aligned} \int p(y_1, \dots, y_{M+1} | x_1, \dots, x_{M+1}) dy_{M+1} &= \int \frac{1}{Z} \int \prod_{i=1}^{M+1} l(y_{\pi_i} | x_{\pi_i}, g \circ \mu_\theta(z)) \exp(-\pi_{\theta'}(z)) \Pi(dz) dy_{M+1} \\ &= \int \frac{1}{Z} \int l(y_{\pi_{M+1}} | x_{\pi_{M+1}}, g \circ \mu_\theta(z)) \prod_{i=1}^M l(y_{\pi_i} | x_{\pi_i}, g \circ \mu_\theta(z)) \exp(-\pi_{\theta'}(z)) \Pi(dz) dy_{M+1} \\ &= \frac{1}{Z} \int \int l(y_{\pi_{M+1}} | x_{\pi_{M+1}}, g \circ \mu_\theta(z)) dy_{M+1} \prod_{i=1}^M l(y_{\pi_i} | x_{\pi_i}, g \circ \mu_\theta(z)) \exp(-\pi_{\theta'}(z)) \Pi(dz) \\ &= \frac{1}{Z} \int \prod_{i=1}^M l(y_{\pi_i} | x_{\pi_i}, g \circ \mu_\theta(z)) \exp(-\pi_{\theta'}(z)) \Pi(dz) \\ &= p(y_1, \dots, y_M | x_1, \dots, x_M). \end{aligned}$$

These two conditions establish that the proposed model defines a valid stochastic process.

B Experiment details

All the experiments was either performed on the CPU or on a RTX 2060 Super. All \mathcal{F} -EBM models took a maximum of 4 hours to train.

B.1 Dataset availability

The datasets can be found online for *Melbourne* (<https://tinyurl.com/rr4vu2b3>) and *GridWatch* (<https://www.gridwatch.templar.co.uk/>). The stocks datasets was collected by querying Investors Exchange (IEX).

B.2 Training and design choices \mathcal{F} -EBM

For all our experiments, we use the same neural architecture and training settings. The setup we use is

- **Architecture.** For the mapping μ_θ , we use a three hidden layered neural network with 512 hidden units and SiLU activations [Elfwing et al., 2018]. We utilize skip connections between the first and second hidden layer, as well as the second and third layer. For the $E_{\theta'}(x)$, we use a similar neural network with 512 hidden layers and SiLU activations with similar skip connections. The key difference is that we use a scaled tanh where the scale is treated as a learnt parameter and clipped to be between $[0, 30]$.
- **Kernel.** We use a Matérn kernel and limit the number of estimated eigenfunction and eigenvalues to be equal to m . Recall that m is the number of evaluation points of each function. We use a similar architecture for
- **Optimization.** We use Adam optimizer with learning rate set to 10^{-3} for μ_θ and 5×10^{-4} with decaying learning rate decay to by a factor of 0.1 when the loss does not decrease. We set the minimum learning rate to be 10^{-5} . We use a batch size of 32 and is ran for 100 epochs with early stopping.

- **Contrastive Divergence.** Contrastive divergence is calculated by samples generated from Stochastic gradient Langevin dynamics with a constant step size of 10^{-3} . We follow with recommendations of Du and Mordatch [2019] and maintain a replay buffer that is sampled from 90% of the time. The MCMC chain is ran for 100 steps.

B.3 Pre-processing

We detail the pre-processing applied to each dataset.

- **Quadratic.** We do not perform any preprocessing for this dataset.
- **Stocks.** We normalize the dataset to have zero mean and unit variance.
- **Gridwatch.** We normalize each sample to have zero mean and unit variance.
- **Melbourne.** We normalize the dataset to have zero mean and unit variance.

B.4 Baseline

- **Gaussian process.** We use the same kernel as \mathcal{F} -EBM, with its parameters obtained from maximising the marginal likelihood.
- **Neural process.** We use a slightly modified version of an implementation of neural processes available online: <https://github.com/EmilienDupont/neural-processes>. We set the dimension of the representation of the context points to be 512 and the dimension of the latent variable to be 512. The encoder and decoder was a 3-layer neural network with 512 hidden units with ReLU activations with the same skip connection. We trained the model up to 1000 epochs with early stopping.
- **π -VAE.** We set the intermediate dimension of the encoder and decoder networks to 100 with ReLU activation, and the dimension of the latent variable to 5. For each dataset the model is trained with early stopping with patience 100. We use the Adam optimizer with a learning rate set to 5×10^{-3} . As feature map $\Phi(\cdot)$ we use a basis representation given by $\Phi(\cdot) = (\phi_1(\cdot), \dots, \phi_B(\cdot))$ where $\{\phi_i(\cdot)\}_{i=1}^B$ is a set of B basis functions. For the basis we compare a Matérn kernel induced basis (m estimated basis functions) with a FPCA based basis (0.99 explained variability) and consequently choose the Matérn kernel induced basis for all datasets except Melbourne. The initial coefficients for the interpolation are estimated from the context pairs via least squares.

C Additional Figures



Figure 4: Samples from the \mathcal{F} -EBM.

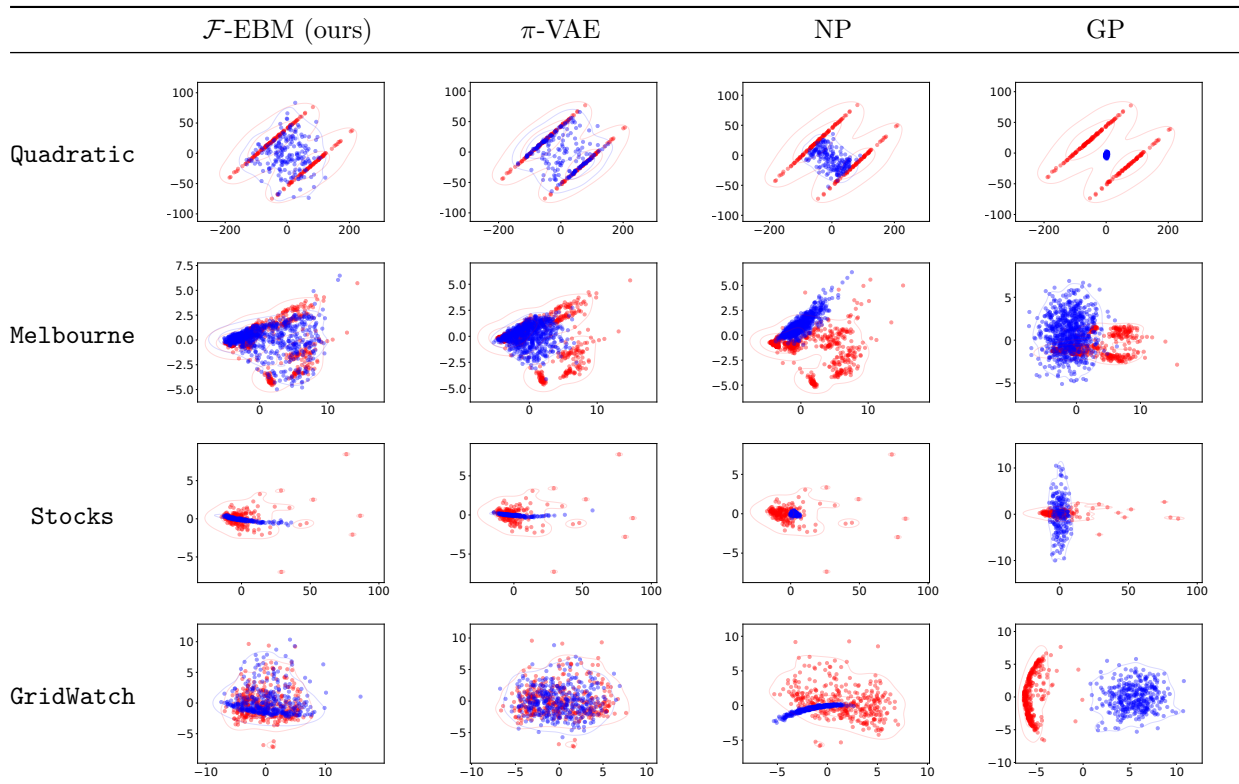


Table 5: The PCA embeddings of 100 samples of both samples generated from the model (blue) and samples from the data (red)